Engineering Journal
issn: 0125-8281

Article

Assessment of Satellite Rainfall Estimates as a Pre-Analysis for Water Environment Analytical Tools: A Case Study for Tonle Sap Lake in Cambodia

Chanarun Phoeurn[a,*] **and Sarann Ly**[b]

Department of Rural Engineering, Institute of Technology of Cambodia, Phnom Penh, Cambodia
Email: [a]Chanarun.p@gmail.com (Corresponding author), [b]ly.sarann@yahoo.com

Abstract. Tonle Sap Lake is the second main source of water supply and food security in Cambodia. However, this area is in the need for rainfall information which can cover the entire area for an accurate hydro-hydraulic modeling, climate modeling and other types of water or environment related modeling. In this case, Satellite Rainfall Estimates (SREs) would play a major role by filling out missing data where gauge observation is not available. The study aims to assess the spatio-temporal performance of two high resolution satellite products such as TRMM 3B42V7 and CHIRPS V.2. One-hundred and fifty four (154) stations around the Tonle Sap Lake and some close to the Mekong River were selected for the analysis within the study period of 2000 to 2004. After this, proper bias correction method is proposed. To do this, GIS and statistical indicators were used for the comparison.

Both TRMM and CHIRPS provide a good correlation with the gauge. Around 90% of stations have CC varies from 0.5 to 0.9. In addition, the median bias of SREs are about 30 mm/month. Both satellite showed very similar pattern of bias spatially and temporally. This can be said that even though TRMM has the lower spatial resolution compared to CHIRPS, the performance of it is better. Moreover, TRMM have higher correlation when each of its cells was compared with the averaging of all stations within that cell. 25% of data that have extreme bias ratio maybe due to other underlying factors such as the distance from the station to the city, the soil elevation, landuse type, age of instrument, occurring of storm or drought that need to be taken into account for the further study.

Keywords: CHIRPS, TRMM, hydraulic modeling, remote sensing, satellite rainfall estimates, Tonle Sap.

ENGINEERING JOURNAL Volume 22 Issue 1
Received 14 September 2017
Accepted 28 October 2017
Published 31 January 2018
Online at http://www.engj.org/
DOI:10.4186/ej.2018.22.1.229

This article is based on the presentation at the THA 2017 International Conference on "Water Management and Climate Change towards Asia's Water-Energy-Food Nexus" in Bangkok, Thailand, 25th-27th January 2017.

1. Introduction

Rainfall is a crucial resource in many socioeconomic activities, and particularly for those countries relying predominantly on rainfed agriculture. Many countries have been affected by rainfall variability and long-term changes in both rainfall amount and distribution over recent decades. After Mekong River, Tonle Sap Lake is the second main source of water supply and food security in Cambodia. However, the number of rain gauges throughout Cambodia is small and unevenly distributed. This is the major challenge for hydro-hydraulic modeling, climate modeling and other types of water or environment related modeling. In this case, Satellite Rainfall Estimates (SREs) would play a major role by filling out missing data where gauge observation is not available. Some global and regional validations have been reported for different satellite rain products [1, 2, 3, 4]. This study aims to use Geographic Information System (GIS) to assess the spatio-temporal performance of two high-resolution satellite products such as TRMM 3B42V7 and CHIRPS versus one-hundred and fifty-four (154) stations within the study period of 2000 to 2004. After this, proper bias correction method is proposed.

2. Study Area

The Kingdom of Cambodia is a country located in the southern portion of the Indochina Peninsula in Southeast Asia. It lies entirely within the tropics, between latitudes 10^{o} and 15^{o}N, and longitudes 102^{o} and 108 ^{o}E. Cambodia's landscape (as showed in Fig. 1) is characterized by a low lying central plain that is surrounded by uplands and low mountains and includes Tonle Sap (Great Lake) and the upper reaches of the Mekong River delta. The most distinct geographical feature is the inundation of the Tonle Sap measuring about 2,590 square kilometers during the dry season and expanding up to 24,605 square kilometers during the rainy season. This densely populated plain, which is devoted to wet rice cultivation, serves as the heartland of Cambodia and much of this area has been designated as biosphere reserved.

Cambodia's climate, like that of the rest of Southeast Asia, is predominantly monsoons, tropical wet and dry seasons. Temperature ranges from 21^{o}C to 35^{o}C (69.8 to 95 ^{o}F) and experiences tropical monsoons. Northeast monsoon is in the dry season, which lasts from November to March. Southwest monsoons blow inland bringing moisture- winds from the Gulf of Thailand and Indian Ocean from May to October. The country experiences the heaviest precipitation from September to October. The driest period occurs from January to February. In Tonle Sap Lake, inundation spatial extents during the dry season is 2,590 square kilometers (1,000 sq mi) and during the dry season is 24,605 square kilometers (9,500 sq mi). Lake Tonle Sap, the largest inland water body in Southeast Asia has a unique ecosystems and wildlife adapted to large seasonal fluctuations in water level. The permanent waterlogged area of the lake is encircled by a vast floodplain. Inundation is in the woodland being dominated by Barringtonia acutangula wood specie. The upstream on the upper Mekong River Monsoon rains during May to Oct. Mean annual rainfall = 1,200-1,300 mm per year.

3. Methodology

One-hundred and fifty four (154) manual raingauges were selected to validate the performance of Satellite Rainfall Estimates (SREs). The data was obtained from the Mekong River Commission (MRC). The stations located in the Tonle Sap basins and some close to the Mekong River (Fig. 2). Since the Mekong River has an important role in the flow regime of the Tonle Sap, stations along it were also selected. The study period is five years. To minimize the seasonal influence, the analyst was made only during the wet months from May to October of 2000 to 2004. We do not have complete data for all the stations during the study period. Thus, we compare only the stations of which data were attainable. Thus, the number of stations is different from year to year as shown in Fig. 3. In this study, we focus only the monthly rainfall. The SREs that were used here are Tropical Rainfall Monitoring Mission (TRMM) 3B42 version 7 and Climate Hazards Group IR Precipitation Station (CHIRPS) version 2.

Fig. 1. Tonle Sap Lake and Mekong River of Cambodia.

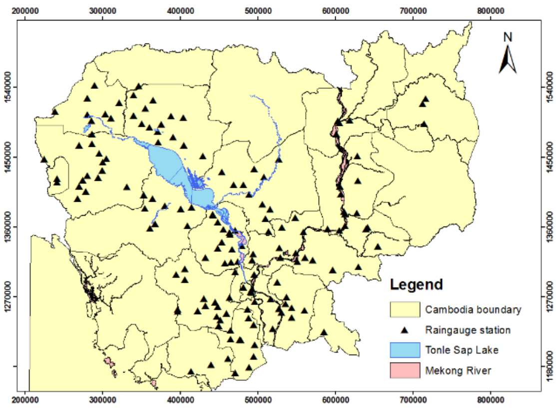

Fig. 2. Location of observed raingauge.

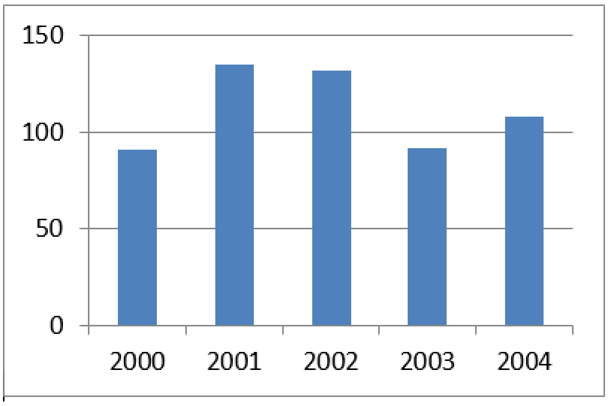

Fig. 3. Number of gauges reported during the studied period.

3.1. Water Accounting Module for CHIRPS and TRMM

The monthly rainfall was downloaded from the Water Accounting Module developed by UNESCO-IHE. The module has daily and monthly rainfall from variety satellites such as TRMM, CHIRPS, and CMORTH converted into the tiff format through "Anaconda" program for Python 2.7 (https://www.continuum.io /downloads). The python code could be access through https://github.com/wateraccounting /wa.

DOI:10.4186/ej.2018.22.1.229

3.2. Spatial Processing in ArcMap 10.4

The intensity of SREs in raster format were extracted and compared with the gauge measurement by using the "Extract Multiple values to points" in the Spatial Analysis toolbox. Aside from this, Geostatistical Analysist was used to display data and identify the outliers. The stations with extremely high value of rainfall were removed. There were two steps for the assessment of SREs performance. First, we compared TRMM and CHIRPS station by station meaning one station per cell. Second, each cell of TRMM (25 km by 25 km) that contains at least two raingauges was selected again for the comparison. Number of gauges varied from 1 to 5 per cell of TRMM. This could not be done for the case of CHIRPS because its resolution is high (4 km by 4 km), thus there were always one raingauge within its cell.

3.3. Description of Satellite Rainfall Estimates

3.3.1. Tropical rainfall monitoring mission (TRMM)

Tropical Rainfall Measurement Mission (TRMM) data provide large-scale estimates of tropical rainfall over the long term. In addition to multispectral visible infrared remote imager (VIRS), microwave imager (TMI), lightning imager, and precipitation radar (PR) instruments, TRMM sensors produce high-quality images that are useful for both the estimation of rainfall and the vertical structure of the hydrometeor fields (through PR and TMI). Table 1 lists a portion of TRMM products [5]. 3B42 version 7 was used for the assessment. It is merged from high quality (HQ)/infrared (IR) precipitation and root-mean-square (RMS) precipitation-error estimates. These gridded estimates are on a 3-hour temporal resolution and a 0.25-degree by 0.25-degree spatial resolution in a global belt extending from 50 degrees South to 50 degrees North latitude. The 3B42 estimates are produced in four stages; (1) the microwave precipitation estimates are calibrated and combined, (2) infrared precipitation estimates are created using the calibrated microwave precipitation, (3) the microwave and IR estimates are combined, and (4) rescaling to monthly data is applied. Each precipitation field is best interpreted as the precipitation rate effective at the nominal observation time [6]. The year of rainfall estimates available for downloading are from 2000 to 2018. The data is in 4-byte binary float from a SUN system and the unit is mm/3hr. Table 1 listed the portion of TRMM products.

3.3.2. CHIRPS

CHIRPS stands for Climate Hazards Group IR Precipitation Station and is a third generation precipitation procedure which is based on various interpolation schemes to create spatially continuous grids from raw point data [7]. The data sources that are used to produce the CHIRPS rainfall product are the monthly precipitation climatology (CHPClim), the IR sensors from the GEO satellites and the MODIS satellite, the TRMM 3B42 product from NASA, and the ground precipitation observations obtained from a variety of sources. First, the precipitation (IRP) is obtained with the use of IR images and the TRMM 3B42 rainfall product for each pentad.

Next, the Cold Cloud Duration (CCD) is calculated. This is determined by summing the total IR observations that are lower than 235K for each pixel. The rain rate is calculated with the following formula:

$$\text{rainrate} = a*CCD+b$$

The TRMM 3B42 product is used to train the monthly models of rainfall and derives the coefficients "a" and "b". The long term IRP means (from 1981 till present) are calculated for each pentad. The current IRP is then divided by the long term IRP means to produce an unitless value that represents the variations in time from the long term mean. A value below 1 means that the rainfall in that pentad was below normal and if this value is higher than 1, than the rainfall was more than average . The resolution of CHIRPS is 0.05^{o}.

Table 1. List a portion of TRMM products.

Product	Description
TRMM 2A12	TRMM 2A25 Contains vertical rainfall-rate profiles, attenuation corrected Z profiles, parameters of Z–R relationships, integrated rainfall rate for each ray, range bin numbers of rain layer boundaries, and many intermediate parameters.
TRMM 2A31	Contains vertical hydrometeor profile derived from PR radar and the 10-GHz channels of the TMI.
TRMM 3A11	Provides monthly oceanic rainfall over 5° lat by 5° long grid box using TRMM TMI data.
TRMM 3B31	Contains 5° x 5° monthly rainfall, adjustment ratio, and hydrometeor profiles
TRMM 3B42	Contains 1° x 1° pentad surface precipitation from the TRMM Combined Product 3B-31 and geosynchronous IR.
TRMM 3B43	Contains 1° x 1° monthly surface precipitation rate from the TRMM Combined Product 3B-31, geosynchronous IR, SSM/I microwave, and rain gauges.

3.4. Statistical Indicators

SREs and observation data was compared spatially and temporally by several statistical indices, including Bias, Relative Bias (RB), Standard Deviation (SD), Root Mean Square Error (RMSE), and Pearson Correlation Coefficients (CC). The definitions of the indicators are described below. The detailed information of the evaluation indices can be found in [8, 9].

$$(B) = \frac{\sum_{n=1}^{N} SREs - Obs}{N} \tag{1}$$

$$(RB\%) = \frac{\sum_{n=1}^{N} SREs - Obs}{\sum_{n=1}^{N} Obs} \times 100 \tag{2}$$

$$RMSE = \sqrt{\frac{1}{N} \sum_{n=1}^{N} (SREs - Obs)^2} \tag{3}$$

$$CC = \frac{\sum_{n=1}^{N} (Obs - \overline{O}) * (SREs - \overline{S})}{SDS * SDO} \tag{4}$$

$$SDs = \sqrt{\frac{1}{N} \sum_{n=1}^{N} SREs - \bar{S}} \tag{5}$$

where N is the number of samples; SREs and Obs stand for individual satellite rainfall and gauge-based estimates, $\overline{S}$ and $\overline{O}$ indicate averaged satellite rainfall and gauge-based estimates, respectively. SDs is the standard deviation of SREs and SDO is the standard deviation of observed rainfall.

3.5. Bias Correction Methods

3.5.1. Spatio-temporal bias correction

This linear bias correction scheme has its origin in the correction of radar based precipitation estimates [10] and downscaled precipitation products from climate models [11, 12]. The bias is corrected for individual raingauge stations at 8 months time step implying that bias correction varies in space and over time, and is based on the use of the B factor estimated from Eq. (6):

$$B = \frac{\sum_{t=1}^{t=8} G(i,t)}{\sum_{t=1}^{t=8} s(i,t)} \tag{6}$$

where G and S = daily gauge and SREs, respectively; i = gauge location. The monthly rainfall estimates are then multiplied by the B for the respective time windows resulting in corrected satellite rainfall estimates in a temporally and spatially coherent manner. The advantages of the bias scheme are the simplicity and modest data requirements and that it adjusts the monthly mean of satellite rainfall at each station.

3.5.2. Distribution transformation

From [13], the bias correction factor for the mean is determined using equation:

$$\mathrm{DT}_{\mu} = \frac{\mathrm{G}_{\mu}}{\mathrm{S}_{\mu}} \tag{7}$$

$$DT_{\tau} = \frac{G_{\tau}}{S_{\tau}} \tag{8}$$

$$S_{AD} = (s_o - s_{\mu})DT_{\tau} + DT_{\mu} \tag{9}$$

$\mathrm{G}_{\mu}$and S_{μ} : mean monthly rainfall of gauge and SRE, respectively;
$G_{\tau} and\ S_{\tau}$: Standard davietion of gauge and SRE, respectively;
S_{AD}: Adjusted value for SRE; S_o: Original value of SRE.

4. Result and Discussion

4.1. Temporal Analysis of SREs versus Observation

4.1.1. Monthly pattern of SREs versus observation

According to Fig. 4, we can be sure that TRMM and CHIRPS captured well the monthly rainfall pattern. May produced the lowest rain rate in the rainy season and August to September were the wettest months. In general, both SREs overestimated the rainfall throughout the year. Figure 4 also revealed that TRMM captured the monthly peaks better than CHIRPS.

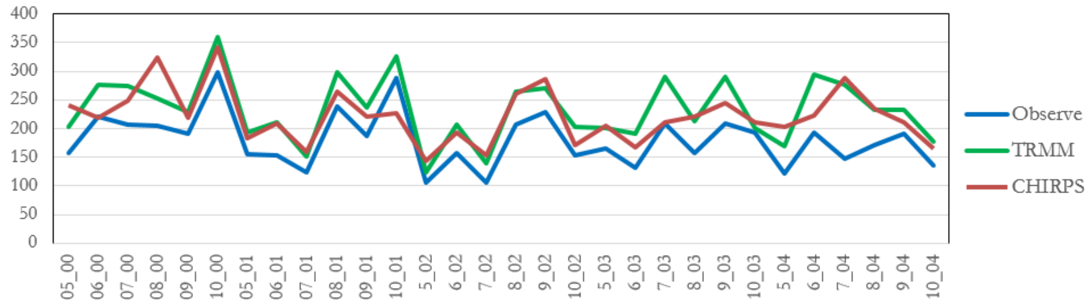

Fig. 4. Average rainfall of gauge and satellites.

Table 2 is the descriptive statistic of (5 yr average) monthly rainfall reported by gauge and satellites. The average monthly rainfall varied from 52.62 to 197.31 mm. Those of TRMM were 39.45 to 169.27 mm and 46.19 to 97.92 mm for CHIRPS, respectively. TRMM estimated less error than CHIRPS. The mean standard daviation of TRMM was 70 mm while the one of CHIRPS was 74 mm. The mean RMSE of TRMM was 94 and was 119 for CHIRPS.

Table 2. Descriptive statistic of (5 yr average) monthly rainfall in mm detected by gauge and satellite.

	Indicator	May	Jun	July	Aug	Sep	Oct
Gauge	Mean	123.18	143.38	145.09	190.73	197.31	208.68
	Min	3.08	3.46	1.20	1.06	0.00	7.44
	Max	399.28	529.82	438.40	629.10	515.06	487.14
	SD	80.74	106.57	95.54	115.12	100.12	96.73
TRMM	Mean	174.70	231.41	224.29	244.04	248.08	254.42
	Min	94.15	120.01	123.62	115.26	143.70	124.08
	Max	397.19	448.86	503.90	526.16	421.65	402.65
	SD	65.66	72.73	73.57	91.88	54.22	61.08
	RMSE	85.93	119.68	102.59	103.68	84.94	88.07

	Indicator	May	Jun	July	Aug	Sep	Oct
CHIRPS	Mean	203.25	209.83	219.23	265.70	243.77	216.18
	Min	110.29	106.22	103.46	103.92	123.29	111.30
	Max	396.23	400.67	502.74	746.52	483.39	397.35
	SD	57.52	65.60	78.87	117.34	68.36	56.64
	RMSE	121.58	120.11	129.99	132.57	112.40	100.07

4.1.2. Monthly correlation

According to Fig. 5, rainfall changes dramatically with time and space. This is similar to the finding of [13] that used CMORPH rainfall estimates in The Zambezi River in Africa. When all the data were pulled together, the correlation became very weak. The mean correlation coefficient was about 0.25 only. However, for spatial pattern, that will be discussed next, the Pearson coefficients were mostly high if stations were compared individually.

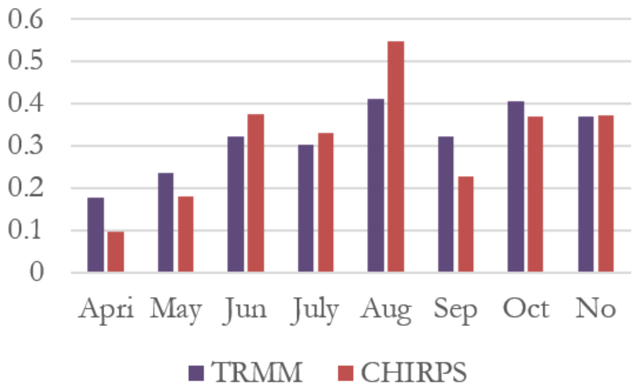

Fig. 5. Pearson correlate coefficient of monthly rainfall.

4.2. Spatial Analyst of SREs versus Observation

4.2.1. Similarity of spatial distribution of both SREs

Figure 6 showed the similarity of TRMM and CHIRPS capturing well the spatial pattern of rainfall over Cambodia. The highest rainfall was located at the South-west part being dominated by coastal and mountainous area. The higher monthly rainfall was at the North-East part of the country consist in the forest and mountain. The middle part of the country around the lake had the lowest rainfall.

DOI:10.4186/ej.2018.22.1.229

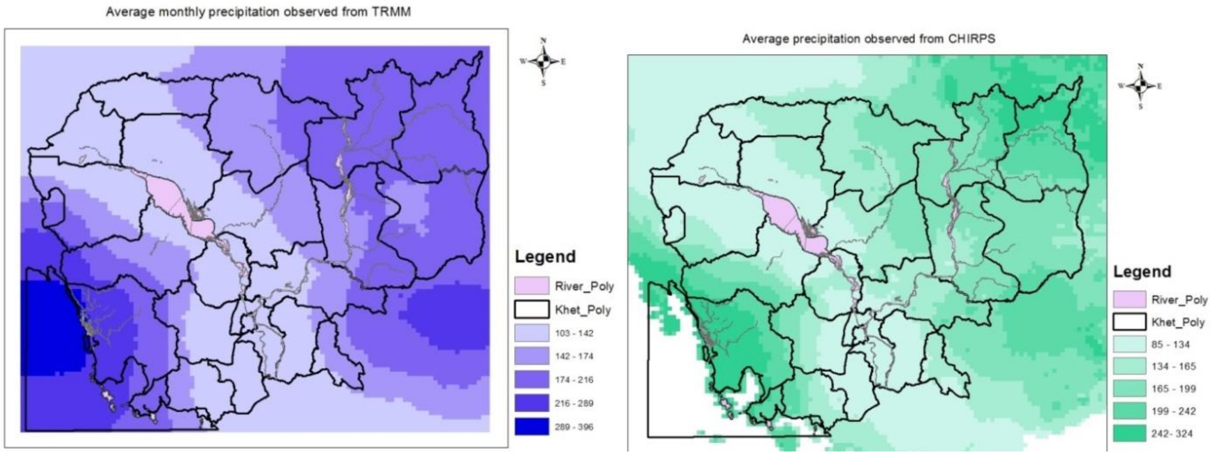

Fig. 6. Spatial distribution of monthly rainfall by TRMM and CHIRPS.

4.2.2. Spatial bias

Both TRMM and CHIRPS showed similar bias patterns distribution in the Tonle Sap and Mekong basins. Figures 7 and 8 indicated the ratio of bias and relative bias for SREs versus gauge values. We can observe that SREs produced high bias in the remote areas and performed better around the lake. This suggested that travel distance could be a challenge for monitoring activities. Elevation could also be the cause. For example, studies such by [14] in Iran demonstrated more accurate estimations of satellite rainfall in highland and mountainous areas than in lowland areas. Contrary, some studies report that satellite rainfall estimations have much smaller error in lowland areas than in mountainous regions [15, 16]. Mostly, the areas of underestimated rainfall by TRMM were identical to those of CHIRPS. Both SREs had similar pattern of bias. One hundred and thirty-eight (138) station measured by TRMM were overestimated from 0.52 to 124 mm/month with the median of 33.11 mm/month. 135 station overestimated by CHIRPS about 0.09 to 116.39 mm/month with the median of 33.94 mm/month.

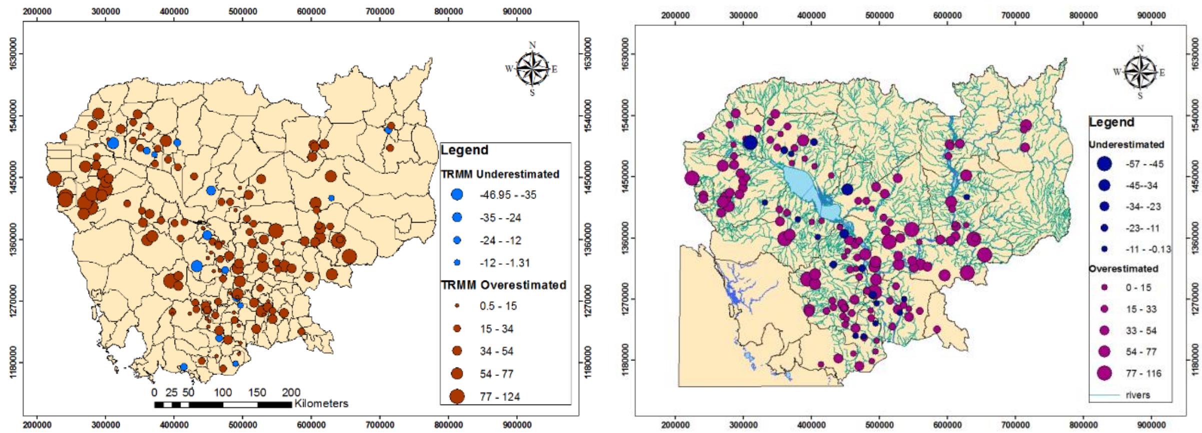

(a) (b)

Fig. 7. (a) Bias for TRMM in mm/month; (b) bias for CHIRPS in mm/month.

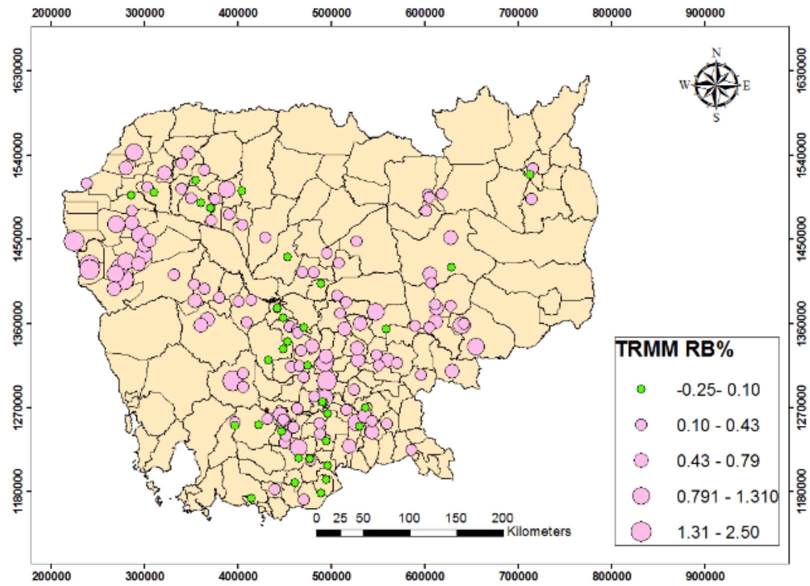

(a)

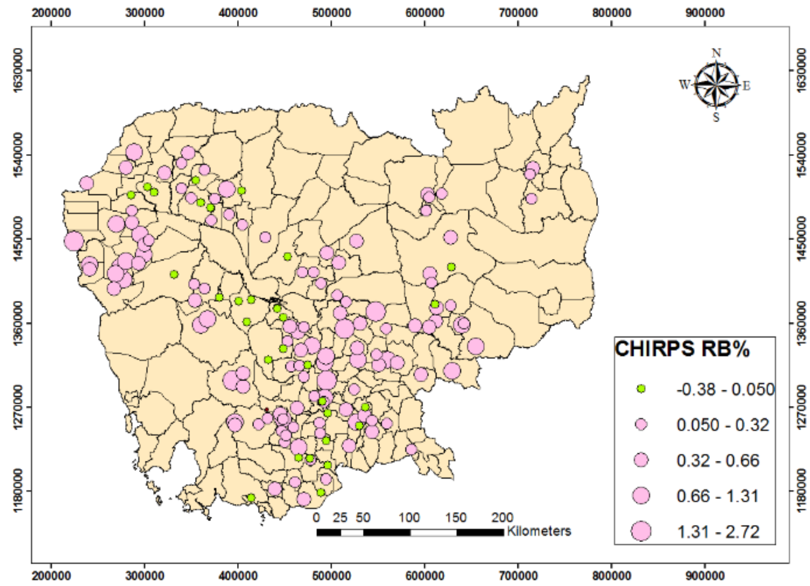

(b)

Fig. 8. (a) Relative bias for TRMM; (b) Relative bias for CHIRPS.

4.2.3. Relative bias

According to Table 3, TRMM had relative bias varied from 0 to 0.92 with the median of 0.32 whereas CHIRPS relative bias varied from 0 to 1.09 with the median of 0.35.

However, the third quartile or 75% of the SREs had the relative bias up to 0.6 and 0.58 only for TRMM and CHIRPS, respectively. This can indicate that the 25% of data that had extreme bias ratio maybe due to the underlying factors that need to be study more including the distance from the station to the city, the soil elevation, the landuse type, the age of instrument, the occurring of storm or drought and the limitation of SREs in certain areas.

Table 3. Relative bias of TRMM and CHIRPS.

	Number of stations	Min	Max	SD	1st Quantile	Median	3rd Quantile
Overestimates							
TRMM	138	0	0.92	0.40	0.16	0.32	0.6
CHIRPS	135	0	1.09	0.42	0.17	0.35	0.58
Underestimates							
TRMM	16	-0.25	0	-0.08	-0.18	-0.14	-0.05
CHIRPS	19	-0.38	0	-0.1	-0.11	-0.07	-0.03

4.2.4. Correlation

According to Fig. 9, 145 out of 154 (94.1%) of TRMM had significant correlated coefficient higher than 0.5 and up to 0.9 indicated strong positive relationship between SREs and observation. The confident level was 95%. Similarly, 146 out of 154 (94.8%) of CHIRPS estimated rainfall that were 0.5 to 0.9 correlated with the gauge base measurement. Both SREs gave similar trend of spatial correlation. However, Fig. 8 demonstrated about better relationship between TRMM and observation.

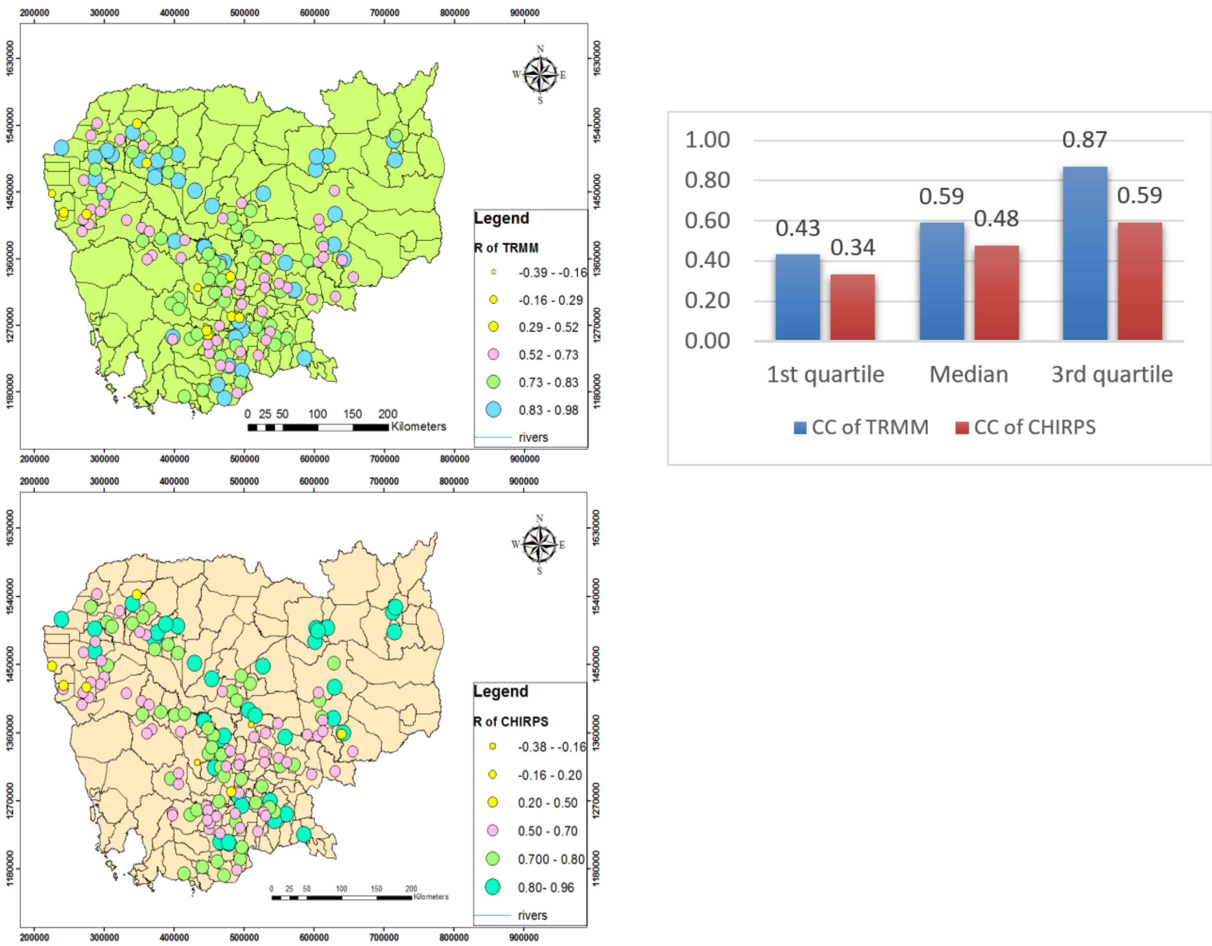

Fig. 9. Correlation of SREs versus observation.

However, Table 4 indicates that TRMM performed much better when its cell was compared with the averaging of all stations within that cell. One should keep this in mind if they want to have a good result from the application of TRMM. The bias of a cell also reduced since it is the mean of the bias from all stations within a cell.

Table 4. Performance of TRMM when being compared differently.

Station code	Compare individually	Average of stations vs. cell	Station code	Compare individually	Average of stations Vs cell
130307	0.61	0.81	120513	0.49	0.46
130311	0.71		120602	0.47	
130306	0.95	0.87	120603	0.24	
130321	0.58		120611	0.56	
130324	0.73		110512	0.40	1.00
120402	0.89	0.88	110513	0.66	
120424	0.65		110519	0.73	
120422	0.42	-0.28	110520	0.47	
120425	0.67		110521	0.61	
120423	0.55	0.53	110524	0.61	
120518	0.45		100419	0.73	0.76
120509	0.78	0.71	100421	0.57	
120515	0.46		110401	0.55	0.79
110526	0.36	0.51	110431	0.74	
110608	0.77		110436	0.72	
110428	0.78	0.82	110403	0.82	0.84
110517	0.81		110419	0.22	
120508	0.66	0.73	120320	0.36	0.36
120520	0.64		120403	0.23	
110423	0.63	0.84	120309	0.42	0.41
110432	0.87		120312	0.26	
110437	0.60		120311	0.13	0.23
110438	0.40		130301	0.36	
110445	0.73	0.87	120206	-0.13	-0.40
110511	0.24		130406	0.01	
110415	0.66	0.60	120202	-0.19	-0.60
110429	0.63		120213	-0.67	
110430	0.43		130304	0.37	0.45
110427	0.46	0.64	130305	0.49	
110449	0.77		130313	0.60	0.68
120301	0.29		130319	0.57	

4.2.5. Bias correction

The SREs corrected by spatio-temporal bias correction method varied from -85 to 30 mm whereas the distribution transformation method created bias from -206 to -22 mm. The latter method underestimated the rainfall and created high error to the original SREs data.

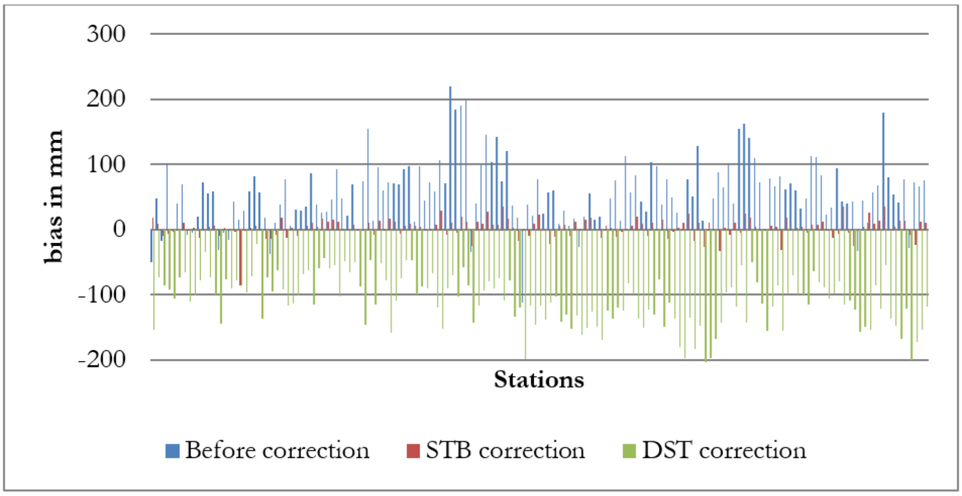

(a)

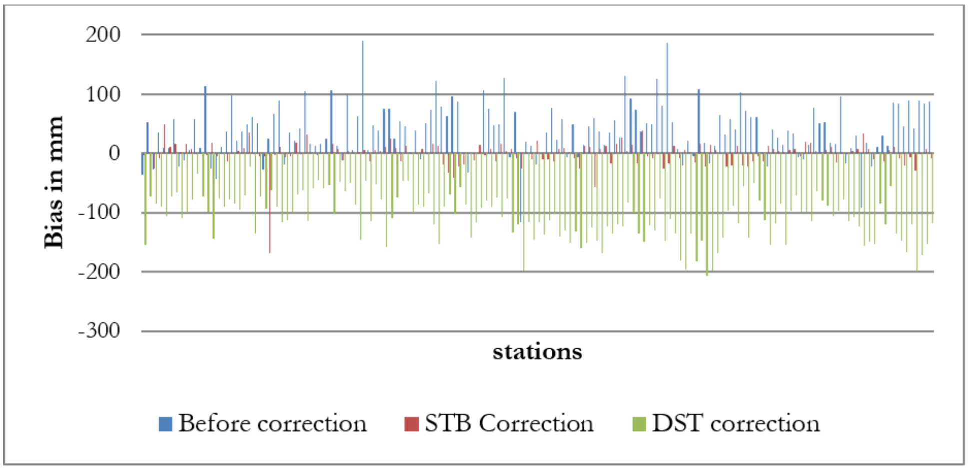

(b)

Fig. 10. (a) Bias of TRMM after correction; (b) Bias of CHIRPS after correction.

5. Summary and Conclusions

Both TRMM and CHIRPS provided a good correlation with the gauge. Around 90% of stations had correlation coefficient varied from 0.5 to 0.9. In addition, the median errors of SREs were about 30 mm/month. Both satellites had the capacity to capture well the rainfall pattern over the study area spatially and temporally. However, TRMM had the better performance though its spatial resolution is lower compared to CHIRPS. TRMM had higher correlation when its cell was compared with the averaging of all stations within that cell. Mostly, both SREs produced similar monthly bias varies around 9 to 70 mm per month and relative bias varied from 0.05 to 0.41 (1 to 3 rd quartile). However, high error for some stations still exist that could be cause due to the distance from the station to the city, the soil elevation, the landuse type, the age of instrument, the occurring of storm or drought and the limitation of SREs in certain areas. These need to be taken into account in the process of bias correction. Finally, both correction methods create the same correlation. The first method is better than the second one.

Acknowledgement

The authors would like also to express high gratitude to JICA and JST through Science and Technology Research Partnership for Sustainable Development, for supporting this research study.

References

[1] S. R. Bajracharya, M. S. Shrestha, and A. B. Shrestha, "Assessment of high-resolution satellite rainfall estimation products in a streamflow model for flood prediction in the Bagmati basin, Nepal," *Journal of Flood Risk Management*, vol. 10, no. 1, pp.5-16, 2014. doi: 10.1111/jfr3.12133

[2] M. J. M. Cheema and W. G. M. Bastiaanssen, "Local calibration of remotely sensed rainfall from the TRMM satellite for different periods and spatial scales in the Indus Basin," International Journal of Remote Sensing, vol. 33, no. 8, pp. 2603-2627, 2012.

[3] M. S. Shrestha, "Bias-adjustment of satellite-based rainfall estimates over the central Himalayas of Nepal for flood prediction," Ph.D. thesis, Kyoto University, 2011.

[4] V. Thiemig, R. Rojas, M. Zambrano-Bigiarini, V. Levizzani, and A. De Roo, "Validation of satellite-based precipitation products over sparsely gauged African river basins," *Journal of Hydrometeorology*, vol. 13, pp. 1760-1783, 2012. doi: 10.1175/jhm-d-12-032.1

[5] S. Sorooshian, K. L. Hsu, X. Gao, H. V. Gupta, B. Imam, and D. Braithwaite, "Evaluation of PERSIANN system satellite-based estimates of tropical rainfall," *Bulletin of the American Meteorological Society*, vol. 81, no. 9, pp. 2035-2046, 2000.

[6] G. J. Huffman, R. F. Adler, P. Arkin, A. Chang, R. Ferraro, A. Gruber, J. Janowiak, A. McNab, B. Rudolf, and U. Schneider, "The Global Precipitation Climatology Project (GPCP) Combined Precipitation Dataset," *Bull. Amer. Meteor. Soc.*, vol. 78, pp. 5–20, 1997.

[7] C. C. Funk, P. J. Peterson, M. F. Landsfeld, D. H. Pedreros, J. P. Verdin, J. D. Rowland, B. E. Romero, G. J. Husak, J. C. Michaelsen, and A. P. Verdin, "A quasi-global precipitatin time series for drought monitoring," US Geological Survey, no. 832, 2013.

[8] E. Ebert, J. Janowiak, and C. Kidd, "Comparison of near-real-time precipitation estimates from satelliteobservations and numerical models," *Bull. Am. Meteorol. Soc.*, vol. 88, pp. 47–64, 2007. doi: 10.1175/BAMS-88-1-47

[9] Y. Tian, C. Peters-Lidard, J. Eylander, R. Joyce, G. Huffman, R. Adler, K. Hsu, F. Turk, M. Garcia, and J. Zeng, "Component analysis of errors in satellite-based precipitation estimates," *J. Geophys. Res.*, vol. 114, no. D24, 2009. doi: 10.1029/JD011949

[10] K. Tesfagiorgis, S. E. Mahani, N. Y. Krakauer, and R. Khanbilvardi, "Bias correction of satellite rainfall estimates using a radar-gauge product—A case study in Oklahoma (USA)," *Hydrol. Earth Syst. Sci.*, vol. 15, pp. 2631-2647, 2011. doi: 10.5194/hess-15-2631-2011

[11] G. Lenderink, A. Buishand, and W. van Deursen, "Estimates of future discharges of the river Rhine using two scenario methodologies: Direct versus delta approach," *Hydrol. Earth Syst. Sci.*, vol. 11, pp. 1145-1159, 2007. doi: 10.5194/hess-11-1145-2007

[12] C. Teutschbein and J. Seibert, "Is bias correction of regional climate model (RCM) simulations possible for non-stationary conditions?," *Hydrol. Earth Syst. Sci.*, vol. 17, pp. 5061-5077, 2013. doi: 10.5194/hess-17-5061-2013

[13] W. Gumindoga, T. H. M. Rientjes, A. T. Haile, H. Makurira, and P. Reggiani, "Bias correction schemes for CMORPH satellite rainfall 2 estimates in the Zambezi River Basin," *Journal Hydrol. Earth Syst. Sci Discuss.*, 2016. doi:10.5194/hess-2016-33

[14] S. Moazami, S. Golian, M. R. Kavianpour, and Y. Hong, "Comparison of PERSIANN and V7 TRMM multi-satellite precipitation analysis (TMPA) products with rain gauge data over Iran," *International Journal of Remote Sensing*, vol. 34, pp. 8156-8171, 2013. doi: 10.1080/01431161.2013.833360

[15] A. S. Gebregiorgis and F. Hossain, "Understanding the dependence of satellite rainfall uncertainty on topography and climate for hydrologic model simulation," IEEE Transactions on Geoscience and Remote Sensing, vol. 51, pp. 704-718, 2013. doi: 10.1109/tgrs.2012.2196282

[16] D. Stampoulis and E. N. Anagnostou, "Evaluation of global satellite rainfall products over continental Europe," *Journal of Hydrometeorology*, vol. 13, pp. 588-603, 2012. doi: 10.1175/jhm-d-11-086.1